



# HOKKAIDO UNIVERSITY

Title	Chromatic dispersion profile optimization of dual-concentric-core photonic crystal fibers for broadband dispersion compensation
Author(s)	Fujisawa, Takeshi; 藤澤, 剛; Saitoh, Kunimasa et al.
Citation	Optics Express, 14(2), 893-900 <a href="https://doi.org/10.1364/OPEX.14.000893">https://doi.org/10.1364/OPEX.14.000893</a>
Issue Date	2006-01-23
Doc URL	<a href="https://hdl.handle.net/2115/5424">https://hdl.handle.net/2115/5424</a>
Rights	© 2006 Optical Society of America, Inc.
Type	journal article
File Information	OE-14-2.pdf



# Chromatic dispersion profile optimization of dual-concentric-core photonic crystal fibers for broadband dispersion compensation

Takeshi Fujisawa, Kunimasa Saitoh, Keisuke Wada, and Masanori Koshiba

*Division of Media and Network Technologies, Hokkaido University, Sapporo 060-0814, Japan*  
[fujisawa@dpo7.ice.eng.hokudai.ac.jp](mailto:fujisawa@dpo7.ice.eng.hokudai.ac.jp), [ksaitoh@ist.hokudai.ac.jp](mailto:ksaitoh@ist.hokudai.ac.jp), [wada@icp.ist.hokudai.ac.jp](mailto:wada@icp.ist.hokudai.ac.jp)  
[koshiba@ist.hokudai.ac.jp](mailto:koshiba@ist.hokudai.ac.jp)

**Abstract:** Chromatic dispersion profile of dual-concentric-core photonic crystal fibers is optimized for broadband dispersion compensation of single mode fibers (SMFs) by using genetic algorithm incorporated with full-vector finite-element method. From the numerical results presented here, it is found that by increasing the distance between central core and outer ring core, larger negative dispersion coefficient and better dispersion slope compensation are possible. There is a tradeoff between the magnitude of negative dispersion coefficient and dispersion slope compensation due to the concave dispersion profile of dual-concentric-core photonic crystal fibers. In spite of the tradeoff, dual-concentric-core photonic crystal fibers having larger negative dispersion coefficient as well as compensating for dispersion slope of SMFs in the entire C band with large effective area can be designed.

©2006 Optical Society of America

**OCIS codes:** (060.2330) Fiber optics communications; (060.2280) Fiber design and fabrication; (999.9999) Photonic crystal fiber

---

## References and links

1. K. Thyagarajan, R.K. Varshney, P. Palai, A.K. Ghatak, and I.C. Goyal, "A novel design of a dispersion compensating fiber," *IEEE Photonics Technol. Lett.* **8**, 1510-1512 (1996).
2. J.-L. Auguste, R. Jindal, J.-M. Blondy, M. Clapeau, J. Marcou, B. Dussardier, G. Monnom, D.B. Ostrowsky, B.P. Pal, and K. Thyagarajan, "–1800 ps/(nm·km) chromatic dispersion of 1.55  $\mu\text{m}$  in dual concentric core fibre," *Electron. Lett.* **36**, 1689-1691 (2000).
3. B.J. Mangan, F. Couny, L. Farr, A. Langford, P.J. Roberts, D.P. Williams, M. Banham, M.W. Mason, D.F. Murphy, E.A.M. Brown, H. Sabert, T.A. Birks, J.C. Knight, and P.St.J. Russel, "Slope-matched dispersion-compensating photonic crystal fibre," in *Proceedings of Conference on Lasers and Electro-Optics (CLEO 2004)*, paper CPDD3, San Francisco, CA, (2004).
4. Y. Ni, L. Zhang, L. An, J. Peng, and C. Fan, "Dual-core photonic crystal fiber for dispersion compensation," *IEEE Photonics Technol. Lett.* **16**, 1516-1518 (2004).
5. F. G r me, J.-L. Auguste, and J.-M. Blondy, "Design of dispersion-compensating fibers based on a dual-concentric-core photonic crystal fiber," *Opt. Lett.* **29**, 2725-2727 (2005).
6. A. Huttunen and P. Torma, "Optimization of dual-core and microstructure fiber geometries for dispersion compensation and large mode area," *Opt. Express* **13**, 627-635 (2005), <http://www.opticsexpress.org/abstract.cfm?URI=OPEX-13-2-627>.
7. B.P. Pal and K. Pande, "Optimization of a dual-core dispersion slope compensating fiber for DWDM transmission in the 1480-1610 nm band through G.652 single-mode fibers," *Opt. Commun.* **201**, 335-344 (2002).
8. F. G r me, J.-L. Auguste, S. F vrier, J. Maury, J.-M. Blondy, L. Gasca, and L. Provost, "Dual concentric core dispersion compensating fiber optimized for WDM application," *Electron. Lett.* **41**, 116-117 (2005).
9. E. Kerrinckx, L. Bigot, M. Douay, and Y. Quiquempois, "Photonic crystal fiber design by means of a genetic algorithm," *Opt. Express* **12**, 1990-1995 (2004), <http://www.opticsexpress.org/abstract.cfm?URI=OPEX-12-9-1990>.
10. F. Poletti, V. Finazzi, T.M. Monro, N.G.R. Broderick, V. Tse, and D.J. Richardson, "Inverse design and fabrication tolerances of ultra-flattened dispersion holey fibers," *Opt. Express* **13**, 3728-3736 (2005), <http://www.opticsexpress.org/abstract.cfm?URI=OPEX-13-10-3728>.

11. T. Fujisawa and M. Koshiba, "Finite element characterization of chromatic dispersion in nonlinear holey fibers," *Opt. Express* **11**, 1481-1489 (2003), <http://www.opticsexpress.org/abstract.cfm?URI=OPEX-11-13-1481>.
  12. K. Saitoh and M. Koshiba, "Full-vectorial imaginary-distance beam propagation method based on a finite element scheme: application to photonic crystal fibers," *IEEE J. Quantum Electron.* **38**, 927-933 (2002).
  13. G.P. Agrawal, *Nonlinear fiber optics*, Academic press (1995).
  14. A. Belahlou, S. Bickham, D. Chowdhury, P.D.A. Evans, J.M. Grochocinski, P. Han, A. Kobayakov, S. Kumar, G. Lutter, J.C. Mauro, Y. Mauro, M. Mlejnek, M.S.K. Muktoyuk, M.T. Murtagh, S. Raghavan, V.R.A. Sevia, N. Taylor, S. Tsuda, M. Vasilyev, and L. Wang, "Fiber design considerations for 40 Gb/s systems," *J. Lightwave Technol.* **20**, 2290-2305 (2002).
  15. G. Renversez, F. Bordas, and B.T. Kuhlmeier, "Second mode transition in microstructured optical fibers: determination of the critical geometrical parameter and study of the matrix refractive index and effects of cladding size," *Opt. Lett.* **30**, 1264-1266 (2005).
  16. K. Saitoh, Y. Tsuchida, M. Koshiba, and N.A. Mortensen, "Endlessly single-mode holey fibers: the influence of core design," *Opt. Express* **13**, 10833-10839 (2005), <http://www.opticsinfobase.org/abstract.cfm?URI=oe-13-26-10833>.
  17. Y. Tsuchida, K. Saitoh, and M. Koshiba, "Design and characterization of single-mode holey fibers with low bending losses," *Opt. Express* **13**, 4770-4779 (2005), <http://www.opticsexpress.org/abstract.cfm?URI=OPEX-13-12-4770>.
- 

## 1. Introduction

Chromatic dispersion of optical fibers is one of the most important parameters for optical communication systems because of its strong influence to temporal optical pulse shape. Specific optical fibers with various dispersion profiles have been proposed such as dispersion flattened fibers, dispersion compensating fibers (DCFs), and so on. In particular, DCFs are indispensable for long distance high speed transmission based on standard single mode fibers (SMFs). To compensate for the accumulated dispersion of SMF after long distance propagation, a dual-concentric-core fiber has been proposed [1],[2]. By introducing outer ring core, it is possible to obtain large negative dispersion coefficient ranging from some hundreds to thousands of ps/(nm·km). To obtain large negative dispersion coefficient, usually a highly Ge-doped central core is required leading to higher losses and fabrication difficulties. To overcome these problems, a dual-concentric-core photonic crystal fiber (DCPCF) has been proposed recently [3]-[6]. It is well known that PCF is very useful for chromatic dispersion management and it is possible to obtain even  $-10000$  ps/(nm·km) dispersion coefficient without Ge doping [5]. However, the available wavelength bandwidth for dispersion compensation of SMF is very narrow because of the concave dispersion profile of dual-concentric-core fibers. Therefore, it is necessary to compensate for the dispersion slope of SMF as well for broadband operation. Although dual-concentric-core fibers with carefully chosen structural parameters have been proposed for broadband dispersion compensation of SMF [7],[8], the problem due to Ge-doping still remains. Huttunen *et al.* reported a DCPCF with high-index core and large air holes which has dispersion values as large as  $-59000$  ps/(nm·km) over a broad wavelength range of 100 nm [6], however, the central core of the proposed DCPCF is not truly single mode and the relative dispersion slope has not been optimized to match with that of a standard SMF in wide wavelength range.

In this paper, chromatic dispersion profile of pure silica DCPCF is optimized for dispersion compensation of a standard SMF in the entire C band (1.53 to 1.565  $\mu\text{m}$ ) by using genetic algorithm (GA) [9],[10] incorporated with full-vector finite-element method (FEM) [11],[12]. From the numerical results presented here, it is found that by increasing the distance between central core and outer ring core, larger negative dispersion coefficient and better dispersion slope compensation are possible. There is a tradeoff between the magnitude of negative dispersion coefficient and dispersion slope compensation due to the concave dispersion profile of DCPCFs. In spite of the tradeoff, single-mode DCPCF having large negative dispersion coefficient as well as compensating for dispersion slope of SMF in the entire C band can be designed.

## 2. Geometries of the DCPCF and genetic algorithm optimization

Here, we consider three types of DCPCFs as shown in Fig. 1, where  $d$  is the hole diameter,  $\Lambda$  is the hole pitch of triangular lattice structure, and the refractive index of background material is given by Sellmeier's equation [13]. The outer ring core is formed by reducing the diameter of air holes in  $i$ -th ring to  $d_r$ . For type 1 (Fig. 1(a)), type 2 (Fig. 1(b)), and type 3 (Fig. 1(c)) DCPCFs,  $i$  is taken as 2, 4, and 6, respectively. It is known that the interference of guided modes of central and ring cores leads to the concave dispersion profile with large negative dispersion coefficient [1].

As an example, Fig. 2 shows chromatic dispersion curves of type 1 DCPCF with  $\Lambda = 2.5 \mu\text{m}$ ,  $d/\Lambda = 0.65$ ,  $d_r/\Lambda = 0.22$  (solid curve), type 2 DCPCF with  $\Lambda = 1.8 \mu\text{m}$ ,  $d/\Lambda = 0.45$ ,  $d_r/\Lambda = 0.25$  (dashed curve), and type 3 DCPCF with  $\Lambda = 1.6 \mu\text{m}$ ,  $d/\Lambda = 0.4$ ,  $d_r/\Lambda = 0.25$  (dash-dot curve). All the dispersion curves presented in this paper is calculated for the fundamental mode of DCPCFs. The concave dispersion profile and large negative dispersion coefficient are clearly seen. The position of concave region can be shifted by tuning structural parameters. We can see that by increasing the distance between the central core and outer ring core (larger values of  $i$ ), larger negative dispersion coefficient can be obtained. If the distance between central core and ring core is small, the guided modes of both cores are strongly coupled and the effective refractive index of the coupled mode is gradually changed with wavelength resulting in smaller negative dispersion coefficient. On the other hand, if the distance is large, the effective refractive index change of the coupled mode is large around the phase matched wavelength leading to larger negative dispersion coefficient.

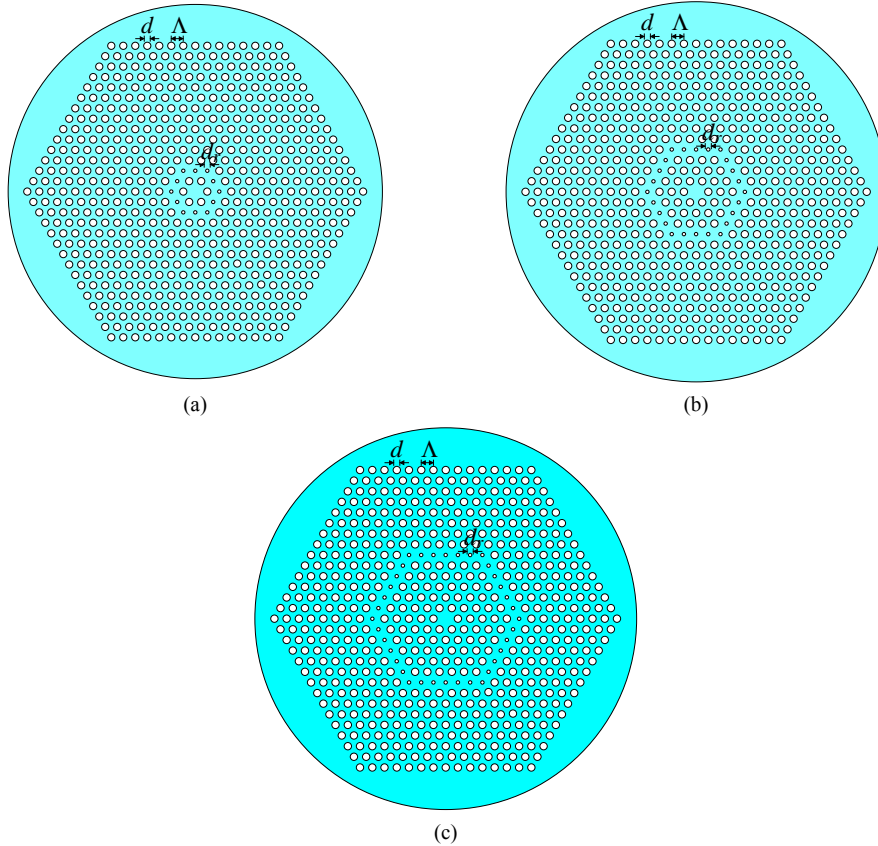


Fig. 1. Cross sections of (a) type 1, (b) type2, and (c) type 3 dual-concentric-core photonic crystal fibers.

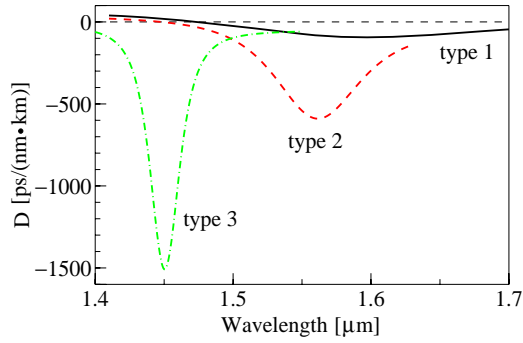


Fig. 2. Dispersion curves of type 1 DCPCF with  $\Lambda = 2.5 \mu\text{m}$ ,  $d/\Lambda = 0.65$ ,  $d_r/\Lambda = 0.22$  (solid curve), type 2 DCPCF with  $\Lambda = 1.8 \mu\text{m}$ ,  $d/\Lambda = 0.45$ ,  $d_r/\Lambda = 0.25$  (dashed curve), and type 3 DCPCF with  $\Lambda = 1.6 \mu\text{m}$ ,  $d/\Lambda = 0.4$ ,  $d_r/\Lambda = 0.25$  (dash-dot curve).

Table 1. Searching areas for each parameter in GA analysis.

Structure	$\Lambda$ [ $\mu\text{m}$ ]	$d/\Lambda$	$d_r/\Lambda$
Type 1	2 to 3	0.4 to 0.8	0.2 to 0.5
Type 2	1.4 to 2	0.3 to 0.7	0.2 to 0.4
Type 3	1.2 to 1.7	0.3 to 0.6	0.2 to 0.4

For the purpose of dispersion compensation, it is advantageous to use concave region because of large negative dispersion coefficient (shorter length of DCPCF) [6]. However, it is difficult to compensate for the dispersion slope of SMF in wide wavelength range because the dispersion profile of SMF is almost linearly varied in C band. To compensate for the dispersion slope of SMF, left hand side of the concave region has to be used in spite of lower negative dispersion coefficient because of smooth and monotonically decreasing dispersion curve. Therefore, there is a tradeoff between the available magnitude of negative dispersion coefficient and dispersion slope compensation. Also, larger effective core area is preferable to reduce splice loss with SMF and nonlinearity in DCF. Designing the dispersion profile having large negative dispersion coefficient, broadband dispersion slope compensation, and large effective core area by trial and error seems to be difficult because the number of required performances and structural parameters to be determined ( $\Lambda$ ,  $d/\Lambda$ , and  $d_r/\Lambda$ ) are large. Therefore, we use GA [9],[10] for designing DCPCF for dispersion compensation of SMF in the entire C band. GA is a kind of optimization algorithm which extracts the best solutions from the given goal. In this case, the best solutions correspond to structural parameters of PCF and the goal corresponds to the target dispersion profiles. Our target dispersion profile is having large negative dispersion coefficient as well as compensating for the dispersion slope of SMF in the entire C band with effective area larger than  $20 \mu\text{m}^2$  at  $1.55 \mu\text{m}$ . The effective area of  $20 \mu\text{m}^2$  is similar to that of conventional dispersion and dispersion slope compensating fibers for compensating standard SMFs. By taking into account these aims, the following fitness function  $F$  is maximized in GA analysis:

$$F(\Lambda, d/\Lambda, d_r/\Lambda) = \exp(w_1 f_1) + f_2 \quad (1)$$

$$f_1 = - \sum_{\lambda=1.53 \mu\text{m}}^{1.565 \mu\text{m}} |D_{\text{target}}(\lambda) + D_{\text{DCPCF}}(\lambda)| \quad (2)$$

$$f_2 = \begin{cases} -0.9 \exp(w_1 f_1) & \text{if } A_{eff@1.55 \mu m} < 20 \mu m^2 \\ 0 & \text{else} \end{cases} \quad (3)$$

where  $w_1$  is a scaling parameter and taken as 0.001,  $A_{eff}$  is the effective core area,  $D_{DCPCF}$  is the dispersion coefficient of DCPCF, and  $\lambda$  is the free-space wavelength.  $D_{target}$  is defined as

$$D_{target}(\lambda) = X \times D_{SMF}(\lambda) \quad (4)$$

where  $X$  is the integer and  $D_{SMF}$  is the dispersion coefficient of SMF.  $f_1$  corresponds to the dispersion slope compensation and if  $D_{SMF}$  is completely compensated by DCPCF,  $f_1$  is zero and  $F$  becomes its maximum value of 1.  $f_2$  is the penalty term with regard to  $A_{eff}$ , and the structure having smaller effective area will be discarded in GA analysis even if it compensates for the dispersion slope of SMF well. Achievable magnitude of negative dispersion coefficient is controlled by  $X$ . If the value of  $X$  is large, DCPCF has to compensate for larger positive chromatic dispersion to maximize  $F$ , and so, DCPCF with larger negative dispersion coefficient will be obtained. However, better dispersion slope compensation is expected for smaller value of  $X$  because of the tradeoff described above. Therefore, the dispersion profile of DCPCF is optimized for several values of  $X$ . Here, FEM modal solver [11],[12] is used for calculating the dispersion profile of DCPCF in the GA analysis ensuring accurate analysis.

Table 2. Optimized structural parameters for type 1 DCPCF and values of  $D_{DCPCF}$  and  $A_{eff}$  at 1.55  $\mu m$ .

$X$	$\Lambda$ [ $\mu m$ ]	$d/\Lambda$	$d_p/\Lambda$	$D_{DCPCF}$ [ps/(nm·km)]	$A_{eff}$ [ $\mu m^2$ ]
5	2.4788	0.6463	0.2180	-88	20.1
10	2.7188	0.7031	0.2069	-180	23.6
20	2.6915	0.7436	0.2106	-347	26.3

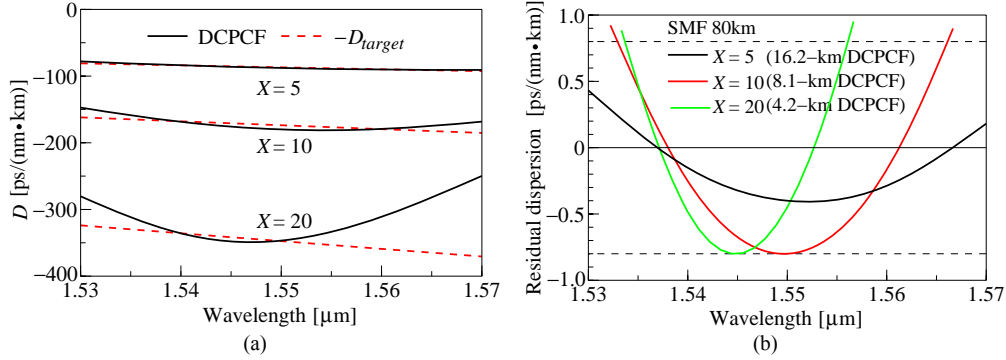


Fig. 3. (a) Optimized chromatic dispersions of type 1 DCPCF for different values of  $X$  and (b) corresponding residual dispersion after compensating for 80-km SMF.

### 3. DCPCF for broadband dispersion compensation

By using the numerical scheme presented in section 2, the dispersion profile of DCPCF shown in Fig. 1 is optimized in terms of  $\Lambda$ ,  $d/\Lambda$ , and  $d_p/\Lambda$ . Searching areas for each parameter are defined from our preliminary calculations and they are summarized in Table 1.

Optimized results for type 1 DCPCF are summarized in Table 2. We can see that  $A_{eff}$  at 1.55  $\mu m$  is larger than 20  $\mu m^2$  for all structures and larger negative dispersion coefficients are obtained for larger values of  $X$  as expected. Although these structures support higher order

modes in the central core region due to the larger values of  $d/\Lambda$ , bending and confinement losses for higher order modes are significantly larger than those of fundamental mode. Therefore, these structures are effectively single-moded in the C band. Figure 3(a) shows optimized chromatic dispersion of type 1 DCPCF for different values of  $X$ . For the sake of eye guideline,  $-D_{target}$  is also shown with red dashed curves. For smaller values of  $X$ , dispersion slope is well compensated in the entire C band, while dispersion slope compensation becomes worse for larger values of  $X$  in spite of larger negative dispersion coefficient resulting in the tradeoff. For larger value of  $X$ , the concave curve can be seen in the dispersion profile. This is because that in DCPCF, the highest negative dispersion coefficient is obtained around the concave region in the dispersion profile. Therefore, optimized results presented here are quite reasonable. It should be noted that the modal field distributions is not Gaussian around the concave region in dispersion curves because of the interference between the central core and the outer ring core modes. Figure 3(b) shows the residual dispersion after compensating for the dispersion of 80-km SMF by optimized type 1 DCPCFs. The lengths of DCPCF are taken as 16.2, 8.1, and 4.2 km for  $X = 5, 10$ , and  $20$ , respectively. The residual dispersion should be lower than  $\pm 0.8$  ps/(nm·km) to compensate for 40 Gb/s signal [14] (dashed lines in Fig. 3(b)). Only the structure for  $X = 5$  meets this condition and the magnitude of negative dispersion coefficient is not so high. Therefore, chromatic dispersions of type 2 and type 3 DCPCFs are optimized for obtaining larger negative dispersion coefficient and better dispersion slope compensation.

Optimized structural parameters for type 2 DCPCF are summarized in Table 3. For larger values of  $X$ , larger negative dispersion coefficient can be obtained and  $A_{eff}$  at  $1.55 \mu\text{m}$  is larger than  $20 \mu\text{m}^2$  for all structures. Figures 4(a) and (b) show optimized chromatic dispersions of type 2 DCPCF for different values of  $X$  and the residual dispersion after compensating for the dispersion of 80-km SMF by optimized type 2 DCPCFs. The lengths of type 2 DCPCF are taken as 16, 8.2, and 4.2 km for  $X = 5, 10$ , and  $20$ , respectively. As can be clearly seen from the figures, the dispersion slope compensation for each structure is better than that of type 1 DCPCFs and the magnitude of negative dispersion coefficient for each value of  $X$  is similar. In this case, all the structures can compensate for 40 Gb/s signal in the entire C band and are endlessly single-mode fibers because of smaller value of  $d/\Lambda$  than  $0.425$  [15],[16].

Table 3. Optimized structural parameters for type 2 DCPCF and values of  $D_{DCPCF}$  and  $A_{eff}$  at  $1.55 \mu\text{m}$ .

$X$	$\Lambda$ [ $\mu\text{m}$ ]	$d/\Lambda$	$d_r/\Lambda$	$D_{DCPCF}$ [ps/(nm·km)]	$A_{eff}$ [ $\mu\text{m}^2$ ]
5	1.8277	0.3409	0.2541	-87	20.7
10	1.8206	0.3757	0.2418	-172	26.6
20	1.8125	0.4202	0.2450	-351	22.9

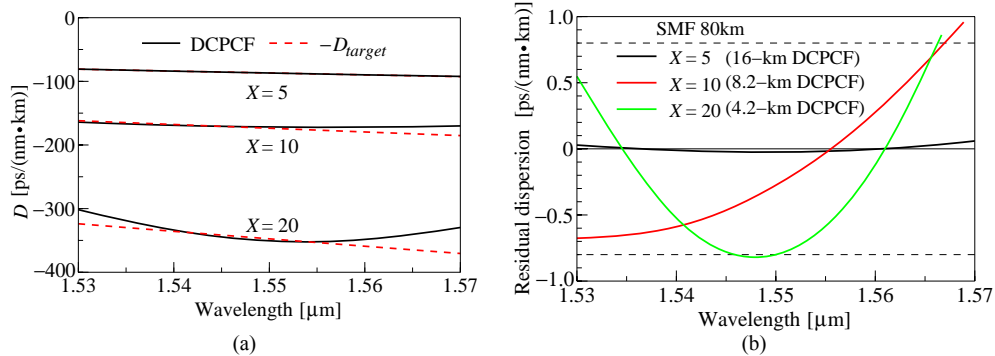


Fig. 4. (a) Optimized chromatic dispersions of type 2 DCPCF for different values of  $X$  and (b) corresponding residual dispersion after compensating for 80-km SMF.

Table 4. Optimized structural parameters for type 3 DCPCF and values of  $D_{DCPCF}$  and  $A_{eff}$  at 1.55  $\mu\text{m}$ .

$X$	$\Lambda$ [ $\mu\text{m}$ ]	$d/\Lambda$	$d_r/\Lambda$	$D_{DCPCF}$ [ps/(nm·km)]	$A_{eff}$ [ $\mu\text{m}^2$ ]
5	1.6945	0.3103	0.2638	-86	25.4
10	1.5356	0.3444	0.2733	-174	23.3
20	1.3853	0.3882	0.2941	-351	21.0
30	1.4633	0.3956	0.2804	-538	23.6

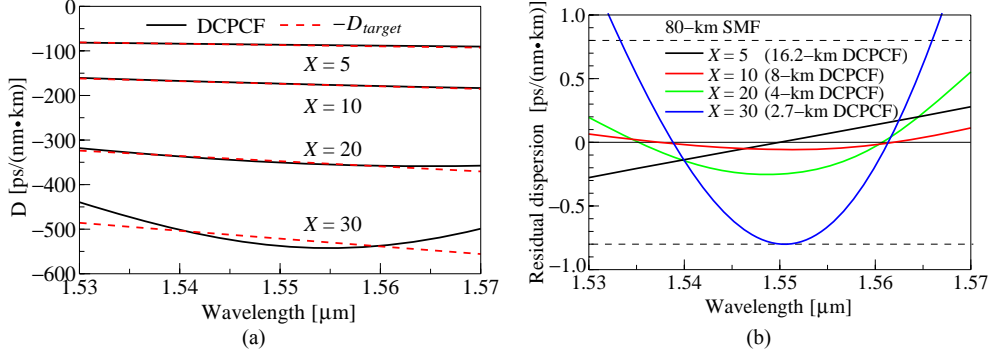


Fig. 5. (a) Optimized chromatic dispersions of type 3 DCPCF for different values of  $X$  and (b) corresponding residual dispersion after compensating for 80-km SMF.

Optimized structural parameters for type 3 DCPCF are summarized in Table 4. For larger values of  $X$ , larger negative dispersion coefficient can be obtained and  $A_{eff}$  at 1.55  $\mu\text{m}$  is larger than 20  $\mu\text{m}^2$  for all structures. Figures 5(a) and (b) show optimized chromatic dispersions of type 3 DCPCF for different values of  $X$  and the residual dispersion after compensating for the dispersion of 80-km SMF by optimized type 3 DCPCFs. The lengths of type 3 DCPCF are taken as 16.2, 8, 4, and 2.7 km for  $X = 5, 10, 20,$  and  $30$ , respectively. Further improvement of dispersion slope compensation compared with those of type 1 and 2 DCPCFs can be clearly seen and single-mode operations are maintained. Structures for  $X = 5, 10,$  and  $20$  can be used for compensating for 40 Gb/s signal over the C band with large negative dispersion coefficient leading to the ultra broadband dispersion compensation. Although the residual dispersion of the structure for  $X = 30$  violates  $\pm 0.8$  ps/(nm·km) condition around 1.53  $\mu\text{m}$ , it can be used in nearly entire C band with very large negative dispersion coefficient (-538 ps/(nm·km) at 1.55  $\mu\text{m}$ ) which is about five times larger than that of commercial dispersion and dispersion slope compensating fibers for C band.

#### 4. Confinement and bending losses

Confinement losses are important and unavoidable problems for all single-material PCF applications. Furthermore, because DCFs are usually installed to the compact package, bending losses are also important issues. Here, confinement and bending losses of the optimized type 3 DCPCF are investigated. The optimized structure for  $X = 30$  ( $\Lambda = 1.4633$   $\mu\text{m}$ ,  $d/\Lambda = 0.3956$ , and  $d_r/\Lambda = 0.2804$ ) is considered. Figure 6(a) shows confinement losses of the optimized DCPCF as a function of the number of air-hole rings at operating wavelengths of 1.53  $\mu\text{m}$  (blue dots), 1.55  $\mu\text{m}$  (green dots), and 1.565  $\mu\text{m}$  (red dots). Confinement losses for this structure are relatively large due to the small values of  $d/\Lambda$  and  $\Lambda$ , and 20 rings of air-holes are required for reducing the confinement losses lower than 0.1 dB/km. However, the required number of air-hole rings can be reduced, for example, by increasing the value of  $d/\Lambda$  in the several outer rings without affecting dispersion characteristics. Figure 6(b) shows

the calculated bending loss (dB/km) of the optimized DCPCF with 20 air-hole rings as a function of bending radius (cm) at operating wavelengths of 1.53  $\mu\text{m}$  (blue dots), 1.55  $\mu\text{m}$  (green dots), and 1.565  $\mu\text{m}$  (red dots). For calculation of the macro-bending induced loss we employ the tilted index model described in [17]. From the results in Fig. 6(b) we can see that even under a drastic bending operation (for bending radii around 1 cm), the corresponding bending losses remain less than 1 dB/km, a result which shows that the optimized DCPCF structure doesn't suffer much from macro-bending losses.

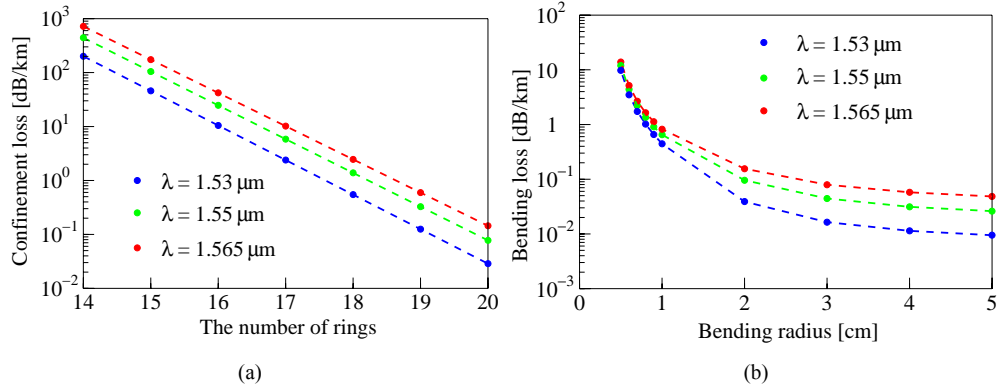


Fig. 6 (a) Confinement losses of the optimized DCPCF as a function of the number of the rings.  
 (b) Bending losses of the optimized DCPCF as a function of bending radius.

## 5. Conclusion

We have optimized the chromatic dispersion of DCPCF for broadband dispersion compensation by using GA incorporated with FEM. It was found from the numerical results presented here that, by increasing the distance between central core and outer ring core, larger negative dispersion coefficient and better dispersion slope compensation can be obtained in the C band. Despite the tradeoff between the magnitude of negative dispersion coefficient and dispersion slope compensation, DCPCF having large negative dispersion coefficient as well as compensating for dispersion slope of SMF in the entire C band was successfully designed.